EXPLORING THE QCD PHASE DIAGRAM WITH FLUCTUATIONS*

Volker Koch

Nuclear Science Division, Lawrence Berkeley National Laboratory
Berkeley, CA, 94720, USA

Volodymyr Vovchenko

Physics Department, University of Houston
Houston, TX 77204, USA

We will discuss how the measurement and calculation of fluctuations of conserved charges, such as the baryon number, may be used to unveil the structure of the QCD phase diagram. We will put special emphasis on how to make the connection between theory and experimental data and what corrections are needed in order to draw meaningful conclusions from experimental measurements.

1. Introduction

One of the open questions concerning the properties of the strong interaction is the existence of a phase transition between hadronic and partonic matter. Such a phase transition, if it exists, would be the only transition potentially accessible to laboratory experiments involving fundamental degrees of freedom of the Standard Model, quarks and gluons. QCD, the theory of strong interactions, is expected to exhibit a second-order $O(4)$ transition in the limit of vanishing quark masses [1], which is related to the chiral symmetry of QCD in this limit. For finite and physical quark masses, however, state-of-the-art lattice QCD calculations [2] have established that at vanishing baryon number chemical potential, the transition from hadrons to quarks and gluons is an analytic crossover. This however does not rule out a phase transition at finite baryon chemical potential. Indeed, model calculations (see [3] for a compilation of various results) as well as recent calculations

using functional methods [4, 5] and Padé extrapolations of lattice QCD [6] results suggest the existence of a critical point associated with a first-order transition at chemical potentials of $\mu_B \gtrsim 600$ MeV.

Experimentally, the QCD phase diagram can be explored through relativistic heavy-ion collisions. Since the location of the transition is expected at finite net-baryon density but its actual position in the baryon density–temperature plane is not known, one needs to carry out a scan in these variables. This can be achieved by varying the collision energy. As the collision energy increases, less and less of the baryons from the projectile and target will be stopped at mid-rapidity. Thus, the net-baryon density of the system at mid-rapidity drops, while at the same time, the temperature increases. Such a scan of the QCD phase diagram is the main motivation of the RHIC beam energy scan program [7, 8]. This program, which provides collisions from $\sqrt{s_{NN}} \simeq 3$–200 GeV, together with the HADES experiment at GSI and future experiments such as CBM, allows to scan a wide range in the temperature–density plane.

Of course, one also needs observables which are sensitive to a possible phase transition. While the usual observables such as spectra, flow, *etc.* may allow to possibly deduce a strong transition, they are at best indirect measures. Fluctuations of conserved charges, baryon number (B), electric charge (Q), and strangeness (S), on the other hand, provide a rather direct sensitivity to the existence of a phase transition or even to some significant changes of the free energy with respect to the control parameters, temperature T and the various chemical potentials μ_i, which are conjugate to the conserved charges. This is because cumulants of distributions of conserved charges measure the derivatives of the grand-canonical partition function, and thus the pressure, with respect to the associated chemical potentials. For example, cumulants of the net-baryon number distribution are given by

$$\kappa_n[B] = \frac{\partial^n}{\partial\,(\mu_B/T)^n} \ln Z = \frac{V}{T} \frac{\partial^n}{\partial\,(\mu_B/T)^n} P\,. \tag{1}$$

Any non-trivial structures in the equation of state such as a possible phase transition [8–11] will result in potentially large derivatives of the pressure which are then reflected in the cumulants of conserved charges. Specifically at the conjectured QCD critical point, cumulants will diverge as powers of the correlation length with higher powers for higher orders of the cumulants [9].

Since cumulants are derivatives of the pressure, they are accessible (at vanishing chemical potential) to lattice QCD calculations [12, 13], which in principle enables a direct comparison of *ab initio* QCD calculations with experiment.

Measurements of fluctuations have meanwhile been carried out by many experiments. The STAR Collaboration has measured cumulants of the net-proton number up to sixth order over the entire energy range available at RHIC [14, 15]. HADES has measured them up to fourth order at an even lower energy of $\sqrt{s} = 2.4$ GeV [16], and ALICE has measured the second- and third-order net-proton cumulant at the LHC at $\sqrt{s} = 2.76$ TeV and 5.02 TeV [17, 18]. NA61/SHINE has charged particle fluctuation over a wide range of energies up to $\sqrt{s} = 17.6$ GeV [19].

When comparing cumulants measured in experiment with those obtained from lattice QCD or other field theoretical calculations [4, 5], one needs to be aware of several key differences. Experiments deal with systems which are finite, evolve in time, and are subject to global conservation laws. Thermal field theory calculations, on the other hand, study static systems in thermal equilibrium and in contact with an infinite heat bath.

In this contribution, we will discuss several of these differences and methods to correct for them. These are essential in order to extract the interesting physics of the QCD phase diagram from heavy-ion experiments. In addition, we will present a non-critical baseline which takes these corrections into account but does not assume any criticality. Such a baseline is important to assess if the data show any hint of possible new physics.

2. Cumulants and factorial cumulants

Since the analysis of fluctuations in heavy-ion collisions is centered around the concept of cumulants, let us remind ourselves about their basic properties. Given a multiplicity distribution $P(N)$, the generating functions for cumulants, $g(t)$, and factorial cumulants, $g_{\mathrm{F}}(t)$, are given by

$$g(t) = \ln\left[\sum_{A,B} P(N)\,\mathrm{e}^{t\,N}\right], \tag{2}$$

$$g_{\mathrm{F}}(z) = \ln\left[\sum_{A,B} P(N)\,z^{N}\right]. \tag{3}$$

By construction, $g(t=0) = 0$ and $g_{\mathrm{F}}(z=1) = 0$. Cumulants and factorial cumulants of the order of k, κ_k, and C_k, are then obtained through

$$\kappa_k = \frac{\partial^k}{\partial t^k} g(t)\bigg|_{t=0}, \tag{4}$$

$$\hat{C}_k = \frac{\partial^k}{\partial z^k} g_{\mathrm{F}}(z)\bigg|_{z=1}. \tag{5}$$

The generating functions, $g(t)$ and $g_{\rm F}(t)$, are related through

$$g_{\rm F}(z) = g\left(\ln(z)\right) \tag{6}$$

which gives rise to simple relations between cumulants and factorial cumulants

$$\kappa_k \;=\; \sum_{j=1}^{k} S(k,j)\hat{C}_j\,, \tag{7}$$

$$\hat{C}_k \;=\; \sum_{j=1}^{k} B_{k,j}\left(1,-1,2,\ldots,(-1)^{j-1}(k-j+1)!\right)\,\kappa_j\,, \tag{8}$$

where $S(k,j)$ denotes the Stirling numbers of the second kind and $B_{k,j}$ are partial Bell polynomials. For the first four orders, this evaluates to

$$\begin{aligned}
\kappa_1 &= \hat{C}_1 = \langle N\rangle\,,\\
\kappa_2 &= \hat{C}_1 + \hat{C}_2\,,\\
\kappa_3 &= \hat{C}_1 + 3\hat{C}_2 + \hat{C}_3\,,\\
\kappa_4 &= \hat{C}_1 + 7\hat{C}_2 + 6\hat{C}_3 + \hat{C}_4\,,
\end{aligned} \tag{9}$$

and

$$\begin{aligned}
\hat{C}_2 &= \kappa_2 - \kappa_1\,,\\
\hat{C}_3 &= 2\kappa_1 - 3\kappa_2 + \kappa_3\,,\\
\hat{C}_4 &= -6\kappa_1 + 11\kappa_2 - 6\kappa_3 + \kappa_4\,.
\end{aligned} \tag{10}$$

In general, cumulants measure the deviation of a distribution from a Gaussian, since for a Gaussian distribution $\kappa_n = 0$ for $n > 2$. And, as already mentioned, cumulants can and have been calculated in finite temperature field theories. This allows for a comparison with experimental data, provided that various caveats and corrections are taken into account, as we shall discuss in more detail below. Factorial cumulants, on the other hand, measure the deviation of a distribution from a Poissonian, since $\hat{C}_n = 0$ for $n > 1$ for a Poisson distribution. In addition, and related to that, factorial cumulants correspond to the integrated irreducible correlation functions. Consider, for example, the one- and two-particle densities, $\rho_1(p_1) = \frac{{\rm d}N}{{\rm d}p_1}$ and $\rho_2(p_1,p_2) = \frac{{\rm d}N}{{\rm d}p_1\,{\rm d}p_2}$. Then the 2-particle density can be written as

$$\rho_2(p_1,p_2) = \rho_1(p_1)\rho_2(p_2) + c_2(p_1,p_2)\,. \tag{11}$$

Here, $c_2(p_1, p_2)$ is the irreducible two-particle correlation function, which typically vanishes if the particles are Poisson distributed[1]. The second-order factorial cumulant is given by

$$\hat{C}_2 = \int \mathrm{d}p_1 \int \mathrm{d}p_2 \, c(p_1, p_2) \,. \tag{12}$$

Analogous relations exist between the higher-order factorial cumulants and correlation functions (see *e.g.*, [8, 20]).

While cumulants have the advantage that they can be calculated in finite temperature field theory, they mix correlations of different orders as can be seen from Eq. (9). This may not be a problem in the ideal situation where we have a singular behavior of the cumulants right at the critical point. In this case, the leading singularities of the cumulants and factorial cumulants are identical as one can also see from Eq. (9) (see also [8]). However, in reality, the lifetime and size of the systems studied in experiment are finite. Therefore, the signal for a critical point is likely just an enhancement of the cumulants. In this case, one expects a slightly larger enhancement of the fourth-order cumulant as compared to the second-order one. However, a similar relative increase may simply be due to a (non-critical) enhancement of the second-order correlation only, since it enters the fourth-order cumulant with a factor of 7. Therefore, a comparison of both, cumulants and factorial cumulants is needed to ensure that any signal is related to critical behavior.

Another advantage of factorial cumulants is that so-called efficiency corrections are readily applied if the efficiency follows a binomial distribution. Consider the factorial cumulant of a distribution $W(n)$ which arises from the folding of the true distributions $P(N)$ with a binomial distribution $B(n, N; \epsilon)$ with Bernoulli probability ϵ, $W(n) = \sum_N B(n, N; \epsilon) P(N)$. Then the factorial cumulants are simply related via

$$\hat{C}_k[W] = \epsilon^k \hat{C}_k[P] \,, \tag{13}$$

where $\hat{C}_k[W]$ and $\hat{C}_k[P]$ are the factorial cumulants for W and P, respectively. Equation (13) together with the relation between cumulants and factorial cumulants then demonstrates that in the limit of $\epsilon \to 0$, all cumulants approach the Poisson limit, $\kappa_n = \langle N \rangle$.

One disadvantage of factorial cumulants is that they can be only reasonably defined for distributions which have only a positive support. In other words, a distribution $P(x)$ which is defined for both positive and negative x, such as the distribution of net baryons cannot be easily discussed in terms of factorial cumulants (see discussion in [20]).

[1] One could imagine a situation where $c_2(p_1, p_2)$ is different from zero, but where its integral vanishes. However, the authors are not aware of any real example where this is the case.

Finally, (factorial) cumulants are extensive quantities, *i.e.*, they scale with the size of the system. Since it is difficult to constrain the size of the systems created in heavy-ion collision, one customarily studies ratios of (factorial) cumulants where the overall system size drops out. However, these still suffer from event-by-event fluctuations of the system size which cannot be fully removed by even the tightest centrality cuts (see Refs. [21–25]).

3. Comparing theory with experiment

As already mentioned in the Introduction, a comparison of cumulants extracted from theory such as lattice QCD calculations with those measured in experiment should be done with some care. Several issues need to be addressed for such a comparison to be meaningful[2]:

— *Global charge conservation:* Finite temperature theory calculations are commonly done in the grand-canonical ensemble, where the system can exchange conserved charges with the external (infinite) heat bath. Thus, the charges such as baryon number, B, strangeness, S, and electric charge, Q, are conserved only on the average. In a heavy-ion collision, the charges of the entire system, on the other hand, are conserved. While one can mimic a grand-canonical ensemble by considering only a subsystem, typically by looking only at slices in rapidity [26], effects of global charge conservation remain since the entire system is still finite. Corrections due to global charge conservation can be quite sizable [27–30]. While most estimates of these corrections are based on the (ideal) hadron resonance gas, recently it has been shown that these corrections can be calculated for *any* equation of state, in particular that of QCD [31–33]. For the commonly used cumulant ratios, one finds

$$\frac{\kappa_2[B]}{\kappa_1[B]} = (1-\alpha)\,\frac{\chi_2^B}{\chi_1^B}\,, \tag{14}$$

$$\frac{\kappa_2[B]}{\kappa_1[B]} = (1-2\alpha)\,\frac{\chi_3^B}{\chi_2^B}\,, \tag{15}$$

$$\frac{\kappa_4[B]}{\kappa_2[B]} = (1-3\alpha\beta)\,\frac{\chi_4^B}{\chi_2^B} - 3\alpha\beta\left(\frac{\chi_3^B}{\chi_2^B}\right)^2\,. \tag{16}$$

Here, $\kappa_n[B]$, represents the baryon number cumulant of the order n, *corrected* for global baryon number conservation. χ_n^B denotes the n^{th}-order baryon number susceptibility, $\frac{\partial^n}{\partial\,(\mu_B/T)^n}P$, for a grand-canonical ensemble in full QCD, as for example determined by lattice QCD.

[2] Here, we will not discuss the important corrections due to volume fluctuations as they will be covered in [21].

The factor α denotes the fraction of the total baryon number which is actually observed, $\alpha = \frac{\langle N_B \rangle_{\text{observed}}}{\langle N_B \rangle_{4\pi}}$, and $\beta = 1 - \alpha$. Since usually one only measures protons, $\alpha < \frac{1}{2}$. We note that the expressions in Eqs. (14)–(16) are valid in the limit where the correlation length is small compared to the system under consideration. As discussed in detail in [31], this is the case for the systems studied in heavy-ion collisions. Similar expressions have also been derived for the other conserved charges, Q and S, as well as for mixed cumulants [32].

— *Thermal smearing:* The above relations between measured cumulants and those obtained in the grand-canonical ensemble do not take into account thermal smearing, *i.e.*, the fact that due to thermal motion even for a boost invariant system, particles in a given spatial rapidity bin are smeared over a range in momentum-space rapidities. As a result of the thermal smearing, the observed cumulants approach the Poisson limit as the acceptance in rapidity approaches zero [34].

— *Baryons vs. protons:* Protons are baryons but not all baryons are protons. Thermal field theory calculations can typically only calculate baryon number susceptibilities as they are associated with the derivative of the pressure w.r.t. the baryon number chemical potential. Experiments, on the other hand, usually cannot measure neutrons and are thus restricted to net-proton number cumulants. As argued in Refs. [35, 36], in the presence of many pions, charge exchange reactions effectively randomize the proton and neutron numbers. In this case, the proton cumulants can be obtained from the baryon-number cumulants by a binomial folding with a Bernoulli probability of $p = \langle N_p \rangle / \langle N_B \rangle \simeq 1/2$. As discussed in the previous section such a binomial folding moves the cumulants closer to the Poisson (Skellam) limit.

The effect of these three corrections is illustrated in Fig. 1 where we show the dependence of the cumulant ratios κ_4/κ_2 and κ_6/κ_2 as a function of the size of the rapidity acceptance window for a typical system produced at LHC energies (for details, see [37]). Here, the horizontal gray lines represent the value for the cumulant ratio as obtained from lattice QCD [13, 38]. The black dashed lines show how this cumulant ratio changes with ΔY due to global charge conservation. The red lines are the result for the cumulant ratio if both charge conservation and thermal smearing are taken into account. Here one sees that, due to thermal smearing, the cumulant ratio approaches the Poisson limit of $\kappa_4/\kappa_2 = 1$ as the acceptance window becomes small. Finally, the blue points show the cumulant ratio for net-protons instead of net baryons with both charge conservation and thermal smearing included.

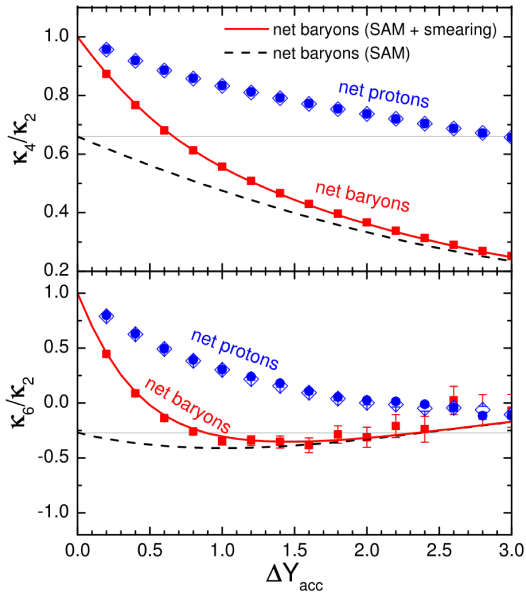

Fig. 1. Cumulant ratio κ_4/κ_2 (upper panel) and κ_6/κ_2 (lower panel) as a function of the acceptance window in rapidity, ΔY, for a system created in heavy-ion collisions at the LHC. The horizontal gray lines represent the result from lattice QCD calculations for the net baryons [13, 38]. The black dashed lines show the effect of global charge conservation, while the red lines include also thermal smearing. The blue points are the results for the net-proton cumulant ratio, again with charge conservation and thermal smearing included. The blue diamonds are the results for net-proton cumulants using the method of [35, 36]. For details, see [37] where this figure is adapted from.

The blue diamonds are the net-proton cumulants obtained using the method of [35, 36]. The blue points are what an experiment such as ALICE is expected to observe if the system created is in thermal equilibrium and if there are no effects other than the fluctuations predicted by lattice QCD. For both cumulant ratios, we see a substantial difference between the predicted value from lattice QCD and what is measured in the experiment using net protons. In particular, for the hyper-kurtosis, κ_6/κ_2, lattice QCD predicts a negative value, while that for net protons turns out to be positive. A negative sign of the hyper-kurtosis has been argued to be a signal for the remnant of chiral criticality [39]. Therefore, great care needs to be taken to reveal the underlying baryon cumulants from those measured. Such an endeavour will likely require the measurement of several cumulant ratios as a function of the size of the acceptance window in order to minimize the systematic uncertainties.

In addition to the aforementioned issues, one should also be aware that the systems created in heavy-ion collisions are dynamic, *i.e.*, they evolve with time whereas the systems studied in thermal field theories are static and in thermal equilibrium. Of course, if the time evolution of the system created in heavy-ion collisions is governed by hydrodynamics and the typical hydrodynamic scale is larger than the correlations length responsible for critical fluctuations as argued *e.g.*, in [40], then the application of (local) thermal equilibrium may be a reasonable approach. If one wants to calculate the effect of critical fluctuation, diffusion and non-hydro modes need to be propagated as well. This can be done either via stochastic hydrodynamics [42] or by explicitly propagating two and higher-order critical correlation functions as proposed in [40] (see also a contribution by Stephanov to these proceedings [41]).

At lower collision energies, which correspond to systems at higher net-baryon density but lower-energy density, non-equilibrium effects are expected to become relevant, so that approaches based on hydrodynamics may no longer be reliable. Instead, one has to resort to some kind of kinetic theory, which has not yet been developed for QCD matter. However, in order to develop some intuition about the importance of non-equilibrium effects and the possibility to detect signals for a dynamical system, it may be a good first step to study classical molecular dynamics. This has been recently done in Refs. [43, 44] for a Lennard-Jones fluid which does have a critical point in the same universality class as the conjectured QCD critical point. This study also addressed, at least qualitatively, another important difference between theory and experiment:

— *Theory calculates in coordinate space while experiment measures in momentum space:* In thermal field theory, one works in the grand-canonical ensemble. In practice, this means that one considers a system with *spatial* sub-volume V_S of a large total volume V_T such that $V_S \ll V_T$. The thermodynamic limit then corresponds to the limit where both volumes go to infinity, V_S, $V_T \to \infty$ while still preserving that $V_S \ll V_T$. Let us, therefore, consider the situation where V_T is large but not infinite. In the limit of $V_S \ll V_T$ but $V_S \gg \xi^3$, one recovers, after suitable corrections for global charge conservation as discussed above, the grand-canonical results for the cumulants. Here, ξ denotes the relevant correlation length. Thus, in theory, one studies the fluctuations of a small *spatial* sub-volume which does particle and energy exchange with the large total volume. At the same time, one integrates over all particle momenta in the small sub-volume. In experiment, the situation is just the opposite: One studies the cumulants of a small sub-volume in *momentum* space characterized by, for example, cuts in rapidity. At the same time, experimental measurements inte-

grate over all coordinate space. This can lead to quite different results as demonstrated in [43]. To see this, let us consider a non-relativistic system, such as the Lennard-Jones fluid which is governed by a two-particle interaction in coordinate space, $V(x_i - x_j)$. The Hamiltonian of such a system is

$$H = \sum_i \frac{p_i^2}{2m} + \sum_{i,j} V(x_j - x_j) \tag{17}$$

so that partition function for a system of N particles in a total phase-space volume $\Omega = \Delta P \times \Delta R$ is given by

$$\begin{aligned} Z &= \int_\Omega \mathrm{d}x_1\, \mathrm{d}p_1 \cdots \mathrm{d}x_N\, \mathrm{d}p_N \exp\left(-\frac{H}{T}\right) \\ &= \int_{\Delta P} \mathrm{d}p_1 \cdots \mathrm{d}p_N \exp\left(-\frac{\sum_i p_i^2}{2mT}\right) \\ &\quad \times \int_{\Delta R} \mathrm{d}x_1 \cdots \mathrm{d}x_N \exp\left(\frac{-\sum_{i,j} V(x_i, x_j)}{T}\right) \\ &= Z_P Z_R\,. \end{aligned} \tag{18}$$

Obviously, the partition function factorizes in a spatial, Z_R, and momentum, Z_P, piece with

$$Z_R = \int_{\Delta R} \mathrm{d}x_1 \cdots \mathrm{d}x_N \exp\left(-\frac{\sum_{i,j} V(x_i, x_j)}{T}\right), \tag{19}$$

$$Z_P = \int_{\Delta P} \mathrm{d}p_1 \cdots \mathrm{d}p_N \exp\left(-\frac{\sum_i p_i^2}{2mT}\right). \tag{20}$$

If we integrate over all momenta but limit the size of the spatial volume, as it is done in theory, we study the behavior of Z_R and are sensitive to the correlations introduced by the interaction. If, on the other hand, we limit the momentum space but integrate over the entire spatial volume as it is done in experiment, the resulting partition function $Z \sim Z_P$ is essentially that of a gas of non-interaction particles. Therefore, one will not observe any non-trivial correlations and fluctuations. Exactly this has been demonstrated in Ref. [43] by explicit simulations of the Lennard-Jones liquid. Thankfully, the systems created in heavy-ion collision are not static but exhibit considerable collective

flow, especially at high energies. Therefore, momentum space and coordinate space are correlated, and cuts in momentum space correspond to some cuts in coordinate space. However at lower energies, where the collective flow is rather modest, one should expect that the signals will become weaker simply because one is approaching the above-discussed static limit. To which extent this is the case that has been studied in [44] for the Lenard-Jones liquid.

4. Non-critical baseline

In order to see if there are any hints or signals from a possible phase transition or critical point in the measured cumulants, one needs a baseline which uses an equation of state without any phase transition but includes all the effects and corrections discussed in the previous section. There are several versions of this in the literature. The STAR Collaboration [14, 15] typically uses the UrQMD event generator for this purpose. UrQMD conserves all the charges, such as the baryon number, and, being based on kinetic theory, includes the effects of thermal smearing. In addition, it provides results for (net) proton cumulants in addition to (net) baryon cumulants. Also, UrQMD being an event generator, one can apply the same acceptance cuts and centrality selection criteria as in the experiment. The latter may help to simulate the effect of volume fluctuations [15]. Another approach [45] uses the hadronic resonance gas including global charge conservation effects and experimental data to constrain the fraction of baryons in the acceptance. Since this approach is based on an ideal gas of hadrons, thermal smearing is automatically included, and the model also gives results for (net) protons. A third approach [46] uses viscous hydrodynamics for the time evolution combined with a particlization method which respects global baryon-number conservation also for (net) protons [33] and, by constructions, includes the effects of thermal smearing. In addition, sampling is done such that the resulting cumulants agree with those from lattice QCD at vanishing chemical potential. This is achieved by introducing an excluded volume correction into the hadron resonance gas equation of state tuned to reproduce the lattice cumulants. Using an excluded volume is justified by an analysis of lattice results for the fugacity expansion of the pressure [47, 48]. However, both this approach and that based on the hadron resonance gas presently do not account for volume fluctuations.

The results for cumulants (left panels) and factorial cumulants (right panels) from the third approach are shown in Fig. 2 together with the data from the STAR Collaboration. Note that the data and calculations are for protons (red lines and symbols) and anti-protons (gray lines and symbols) separately, but not for net protons. The solid lines represent the results

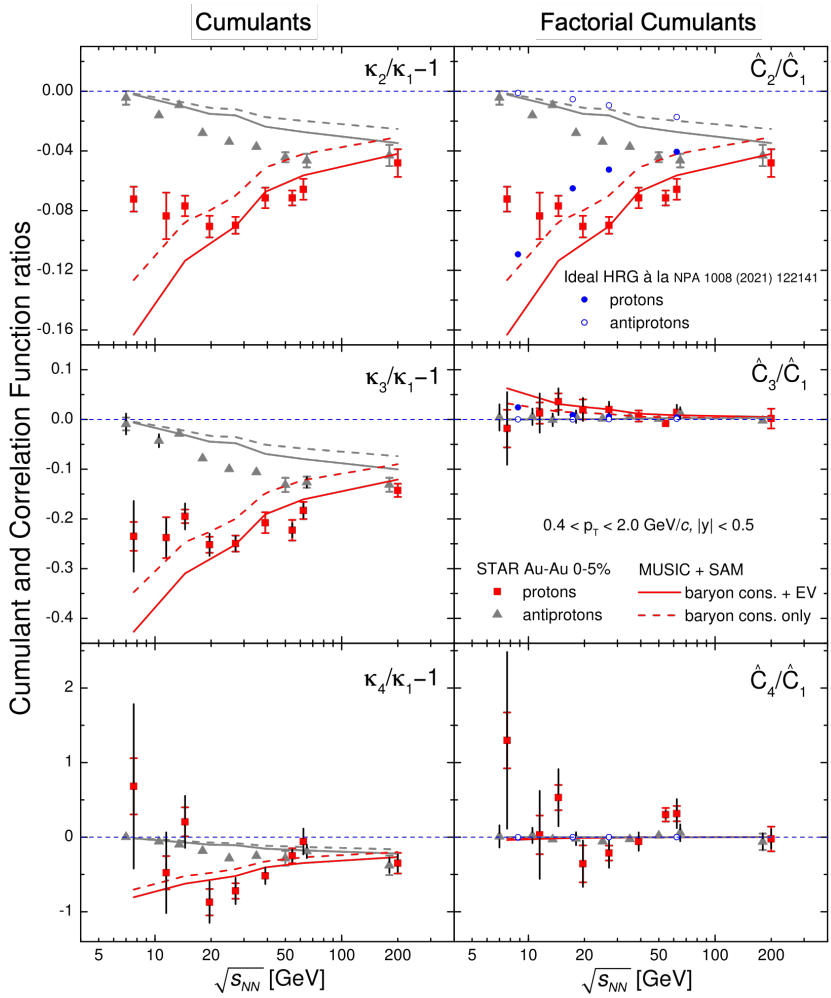

Fig. 2. Comparison of STAR data with the non-critical baseline calculated in [46] for cumulants and factorial cumulants. Data are from Ref. [14]. The figure is adapted from [46].

using the excluded volume correction for the sampling process. The dashed lines are the results without these corrections and are very similar to those of Ref. [45]. We find that for collision energies above $\sqrt{s_{NN}} \simeq 20$ GeV, the baseline agrees well with the data for all proton (factorial) cumulants. This is not the case for the anti-protons, a discrepancy which remains an open question. We further observe that the third- and fourth-order factorial cumulants are (within errors) consistent with this baseline. For the second-order factorial cumulant, on the other hand, the baseline significantly underpredicts the data for energies below $\sqrt{s_{NN}} \simeq 15$ GeV. The third- and fourth-order

cumulants also seem to show some discrepancy between data and baseline. However, this difference has its origin in that of the second-order factorial cumulant. As discussed in the previous section, cumulants are a superposition of the factorial cumulants (see Eq. (9)) so that the discrepancy of the second-order *factorial* cumulant enters the higher-order cumulants. This is a nice example which demonstrates that looking at cumulants only may lead to wrong impressions.

Given the presently available data, there is a clear deviation of the data from the baseline for the second order cumulants which persists and actually increases at even lower energies as shown in Fig. 3. One cause for this difference may be volume fluctuations. As shown in [49] the second order factorial cumulants receive the strongest contribution from volume fluctuations. In addition, at lower energies the multiplicity of charged particles, which is used for centrality selection, is lower, resulting in less precise centrality determination. Therefore, it would be interesting to see how the new methods for removing volume fluctuations proposed in Refs. [24, 25] and discussed in the contribution by Rustamov [21] change the present data. In any case given the large discrepancy between the data and the baseline for the second order (factorial) cumulants it seems wise to understand those first before interpreting the higher order cumulants in terms of any critical dynamics. And, given the rather large error bars of the higher order cumulants it may be good to wait for the data from second phase of the RHIC beam energy scan, which will have much improved statistics.

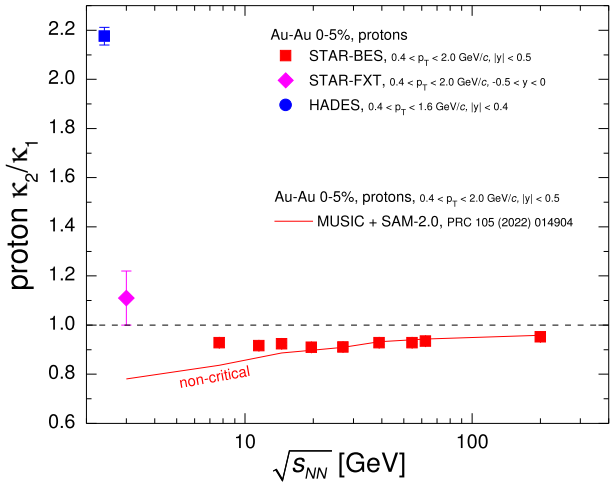

Fig. 3. Collision energy dependence of κ_2/κ_1 for protons. The data are from [14, 15] (STAR) and [16] (HADES). The red line represents the non-critical baseline determined in [46].

5. Summary

In summary, we have discussed how the study of fluctuations may help to find interesting structures and possible phase transitions in the QCD phase diagram. The measure of these fluctuations, the cumulants of the distributions of conserved charges, can be calculated in thermal field theories and, with some limitations, can also be measured in experiment. This allows for a direct comparison between the predictions of (lattice) QCD and measurement.

We have emphasized that such a comparison needs to be done with some care as the systems created in heavy-ion collisions are different from those studied in theory. Issues such as global charge conservation, thermal smearing, volume fluctuations, *etc.* need to be carefully accounted for. While this may seem like an impossible task, considerable progress has been made years since these ideas originally have been formulated [9, 26]. The progress has not been restricted to theory and phenomenology. On the experimental side, the quality and wealth of the data have improved significantly. Fluctuation measurements have and will be carried out over the entire collision energy range allowing for a comprehensive understanding of these issues and, more importantly, the physics of the QCD phase diagram.

Finally, we should point out that fluctuations may also help to constrain and measure other interesting properties of dense matter, such as the speed of sound [50] or the rate of baryon annihilation in the hadronic phase [51], just to name a few. Thus, fluctuations measurements and their interpretation, while difficult and challenging, provide rich insights into the properties of the QCD matter created in heavy-ion collisions

We would like to thank M. Gorenstein, V. Kuznietsov, R. Poberezhnyuk, O. Savchuk, C. Shen, and J. Steinheimer for fruitful collaborations which led to the results presented here. This work is supported by the Director, Office of Energy Research, Office of High Energy and Nuclear Physics, Divisions of Nuclear Physics, of the U.S. Department of Energy under contract No. DE-AC02-05CH11231.

REFERENCES

[1] R.D. Pisarski, F. Wilczek, «Remarks on the chiral phase transition in chromodynamics», *Phys. Rev. D* **29**, 338 (1984).

[2] Y. Aoki *et al.*, «The order of the quantum chromodynamics transition predicted by the standard model of particle physics», *Nature* **443**, 675 (2006), arXiv:hep-lat/0611014.

[3] A. Pandav, D. Mallick, B. Mohanty, «Search for the QCD critical point in high energy nuclear collisions», *Prog. Part. Nucl. Phys.* **125**, 103960 (2022), arXiv:2203.07817 [nucl-ex].

[4] W.-j. Fu, J.M. Pawlowski, F. Rennecke, «QCD phase structure at finite temperature and density», *Phys. Rev. D* **101**, 054032 (2020), arXiv:1909.02991 [hep-ph].

[5] J. Bernhardt, C.S. Fischer, P. Isserstedt, «Finite-volume effects in baryon number fluctuations around the QCD critical endpoint», *Phys. Lett. B* **841**, 137908 (2023), arXiv:2208.01981 [hep-ph].

[6] HotQCD Collaboration (D. Bollweg *et al.*), «Taylor expansions and Padé approximants for cumulants of conserved charge fluctuations at nonvanishing chemical potentials», *Phys. Rev. D* **105**, 074511 (2022), arXiv:2202.09184 [hep-lat].

[7] G. Odyniec, «RHIC Beam Energy Scan Program: Phase I and II», *PoS* **(CPOD2013)**, 043 (2013).

[8] A. Bzdak *et al.*, «Mapping the phases of quantum chromodynamics with beam energy scan», *Phys. Rep.* **853**, 1 (2020), arXiv:1906.00936 [nucl-th].

[9] M. Stephanov, «Non-Gaussian Fluctuations near the QCD Critical Point», *Phys. Rev. Lett.* **102**, 032301 (2009), arXiv:0809.3450 [hep-ph].

[10] M. Stephanov, «Sign of Kurtosis near the QCD Critical Point», *Phys. Rev. Lett.* **107**, 052301 (2011), arXiv:1104.1627 [hep-ph].

[11] M. Asakawa, S. Ejiri, M. Kitazawa, «Third Moments of Conserved Charges as Probes of QCD Phase Structure», *Phys. Rev. Lett.* **103**, 262301 (2009), arXiv:0904.2089 [nucl-th].

[12] HotQCD Collaboration (A. Bazavov *et al.*), «Skewness and kurtosis of net baryon-number distributions at small values of the baryon chemical potential», *Phys. Rev. D* **96**, 074510 (2017), arXiv:1708.04897 [hep-lat].

[13] S. Borsanyi *et al.*, «Higher order fluctuations and correlations of conserved charges from lattice QCD», *J. High Energy Phys.* **2018**, 205 (2018), arXiv:1805.04445 [hep-lat].

[14] STAR Collaboration (M. Abdallah *et al.*), «Cumulants and correlation functions of net-proton, proton, and antiproton multiplicity distributions in Au+Au collisions at energies available at the BNL Relativistic Heavy Ion Collider», *Phys. Rev. C* **104**, 024902 (2021), arXiv:2101.12413 [nucl-ex].

[15] STAR Collaboration (M. Abdallah *et al.*), «Higher-order cumulants and correlation functions of proton multiplicity distributions in $\sqrt{s_{NN}} = 3$ GeV Au+Au collisions at the RHIC STAR experiment», *Phys. Rev. C* **107**, 024908 (2023), arXiv:2209.11940 [nucl-ex].

[16] HADES Collaboration (J. Adamczewski-Musch *et al.*), «Proton number fluctuations in $\sqrt{s_{NN}} = 2.4$ GeV Au+Au collisions studied with HADES», *Phys. Rev. C* **102**, 024914 (2020), arXiv:2002.08701 [nucl-ex].

[17] ALICE Collaboration (S. Acharya *et al.*), «Global baryon number conservation encoded in net-proton fluctuations measured in Pb–Pb collisions at $\sqrt{s_{NN}} = 2.76$ TeV», *Phys. Lett. B* **807**, 135564 (2020), arXiv:1910.14396 [nucl-ex].

[18] ALICE Collaboration (S. Acharya *et al.*), «Closing in on critical net-baryon fluctuations at LHC energies: Cumulants up to third order in Pb–Pb collisions», *Phys. Lett. B* **844**, 137545 (2023), arXiv:2206.03343 [nucl-ex].

[19] NA61/SHINE Collaboration (H. Adhikary *et al.*), «Measurements of higher-order cumulants of multiplicity and net-electric charge distributions in inelastic proton–proton interactions by NA61/SHINE», arXiv:2312.13706 [hep-ex].

[20] A. Bzdak, V. Koch, N. Strodthoff, «Cumulants and correlation functions versus the QCD phase diagram», *Phys. Rev. C* **95**, 054906 (2017), arXiv:1607.07375 [nucl-th].

[21] A. Rustamov, «Deciphering Phase Transitions via Event-by-Event Particle Number Fluctuations and Correlation», presented at the LXIII Cracow School of Theoretical Physics *Nuclear Matter at Extreme Densities and High Temperatures*, Zakopane, Poland, 17–23 September, 2023, (pdf).

[22] M.I. Gorenstein, M. Gaździcki, «Strongly intensive quantities», *Phys. Rev. C* **84**, 014904 (2011), arXiv:1101.4865 [nucl-th].

[23] V. Skokov, B. Friman, K. Redlich, «Volume fluctuations and higher-order cumulants of the net baryon number», *Phys. Rev. C* **88**, 034911 (2013), arXiv:1205.4756 [hep-ph].

[24] A. Rustamov, J. Stroth, R. Holzmann, «A model-free procedure to correct for volume fluctuations in E-by-E analyses of particle multiplicities», *Nucl. Phys. A* **1034**, 122641 (2023), arXiv:2211.14849 [nucl-th].

[25] R. Holzmann, V. Koch, A. Rustamov, J. Stroth, «Controlling volume fluctuations for studies of critical phenomena in nuclear collisions», arXiv:2403.03598 [nucl-th].

[26] V. Koch, «Hadronic Fluctuations and Correlations», in: R. Stock (Ed.) «Relativistic Heavy Ion Physics. Landolt-Boernstein New Series I», vol. 23, *Springer, Heidelberg*, 2010, pp. 626–652, arXiv:0810.2520 [nucl-th].

[27] A. Bzdak, V. Koch, V. Skokov, «Baryon number conservation and the cumulants of the net proton distribution», *Phys. Rev. C* **87**, 014901 (2013), arXiv:1203.4529 [hep-ph].

[28] P. Braun-Munzinger, A. Rustamov, J. Stachel, «Bridging the gap between event-by-event fluctuation measurements and theory predictions in relativistic nuclear collisions», *Nucl. Phys. A* **960**, 114 (2017), arXiv:1612.00702 [nucl-th].

[29] O. Savchuk, R.V. Poberezhnyuk, V. Vovchenko, M.I. Gorenstein, «Binomial acceptance corrections for particle number distributions in high-energy reactions», *Phys. Rev. C* **101**, 024917 (2020), arXiv:1911.03426 [hep-ph].

[30] P. Braun-Munzinger, K. Redlich, A. Rustamov, J. Stachel, «The imprint of conservation laws on correlated particle production», arXiv:2312.15534 [nucl-th].

[31] V. Vovchenko *et al.*, «Connecting fluctuation measurements in heavy-ion collisions with the grand-canonical susceptibilities», *Phys. Lett. B* **811**, 135868 (2020), arXiv:2003.13905 [hep-ph].

[32] V. Vovchenko, R.V. Poberezhnyuk, V. Koch, «Cumulants of multiple conserved charges and global conservation laws», *J. High Energy Phys.* **2020**, 089 (2020), arXiv:2007.03850 [hep-ph].

[33] V. Vovchenko, «Correcting event-by-event fluctuations in heavy-ion collisions for exact global conservation laws with the generalized subensemble acceptance method», *Phys. Rev. C* **105**, 014903 (2022), arXiv:2106.13775 [hep-ph].

[34] B. Ling, M.A. Stephanov, «Acceptance dependence of fluctuation measures near the QCD critical point», *Phys. Rev. C* **93**, 034915 (2016), arXiv:1512.09125 [nucl-th].

[35] M. Kitazawa, M. Asakawa, «Revealing baryon number fluctuations from proton number fluctuations in relativistic heavy ion collisions», *Phys. Rev. C* **85**, 021901 (2012), arXiv:1107.2755 [nucl-th].

[36] M. Kitazawa, M. Asakawa, «Relation between baryon number fluctuations and experimentally observed proton number fluctuations in relativistic heavy ion collisions», *Phys. Rev. C* **86**, 024904 (2012); *Erratum ibid.* **86**, 069902 (2012), arXiv:1205.3292 [nucl-th].

[37] V. Vovchenko, V. Koch, «Particlization of an interacting hadron resonance gas with global conservation laws for event-by-event fluctuations in heavy-ion collisions», *Phys. Rev. C* **103**, 044903 (2021), arXiv:2012.09954 [hep-ph].

[38] A. Bazavov *et al.*, «QCD equation of state to $\mathcal{O}(\mu_B^6)$ from lattice QCD», *Phys. Rev. D* **95**, 054504 (2017), arXiv:1701.04325 [hep-lat].

[39] B. Friman *et al.* (Eds.) «The CBM Physics Book Compressed Baryonic Matter in Laboratory Experiments. Lecture Notes in Physics, vol. 814», *Springer*, Berlin, Heidelberg 2011.

[40] M. Stephanov, Y. Yin, «Hydrodynamics with parametric slowing down and fluctuations near the critical point», *Phys. Rev. D* **98**, 036006 (2018), arXiv:1712.10305 [nucl-th].

[41] M. Stephanov, «QCD Critical Point and Hydrodynamic Fluctuations in Relativistic Fluids», *Acta Phys. Pol. B* **55**, 5-A4 (2024).

[42] L.D. Landau, E.M. Lifshitz, «Hydrodynamics, Course of Theoretical Physics, Vol. VI», *Pergamon Press*, New York 1980.

[43] V.A. Kuznietsov *et al.*, «Critical point particle number fluctuations from molecular dynamics», *Phys. Rev. C* **105**, 044903 (2022), arXiv:2201.08486 [hep-ph].

[44] V.A. Kuznietsov, M.I. Gorenstein, V. Koch, V. Vovchenko, «Coordinate versus momentum cuts and effects of collective flow on critical fluctuations», arXiv:2404.00476 [nucl-th].

[45] P. Braun-Munzinger *et al.*, «Relativistic nuclear collisions: Establishing a non-critical baseline for fluctuation measurements», *Nucl. Phys. A* **1008**, 122141 (2021), arXiv:2007.02463 [nucl-th].

[46] V. Vovchenko, V. Koch, C. Shen, «Proton number cumulants and correlation functions in Au–Au collisions at $\sqrt{s_{NN}} = 7.7$–200 GeV from hydrodynamics», *Phys. Rev. C* **105**, 014904 (2022), arXiv:2107.00163 [hep-ph].

[47] V. Vovchenko, J. Steinheimer, O. Philipsen, H. Stoecker, «Cluster expansion model for QCD baryon number fluctuations: No phase transition at $\mu_B/T < \pi$», *Phys. Rev. D* **97**, 114030 (2018), arXiv:1711.01261 [hep-ph].

[48] V. Vovchenko *et al.*, «Repulsive baryonic interactions and lattice QCD observables at imaginary chemical potential», *Phys. Lett. B* **775**, 71 (2017), arXiv:1708.02852 [hep-ph].

[49] A. Bzdak, V. Koch, V. Skokov, N. Strodthoff, «Cumulants vs correlation functions and the QCD phase diagram at low energies», *Nucl. Phys. A* **967**, 465 (2017).

[50] A. Sorensen, D. Oliinychenko, V. Koch, L. McLerran, «Speed of Sound and Baryon Cumulants in Heavy-Ion Collisions», *Phys. Rev. Lett.* **127**, 042303 (2021), arXiv:2103.07365 [nucl-th].

[51] O. Savchuk *et al.*, «Constraining baryon annihilation in the hadronic phase of heavy-ion collisions via event-by-event fluctuations», *Phys. Lett. B* **827**, 136983 (2022), arXiv:2106.08239 [hep-ph].